Hussar converted-wave data processing and analysis

J. Helen Isaac and John C. Bancroft

ABSTRACT

We processed and inverted converted-wave data acquired during the low-frequency shoot at Hussar, Alberta in September, 2011. The two datasets we selected were generated from dynamite and low-dwell vibroseis sources and were recorded on 3C 10 Hz geophones. The data processing included radial filtering and Gabor deconvolution. The stacked dynamite and vibroseis data both show strong converted-wave reflections. Receiver statics were derived successfully by flattening an horizon picked on a stack of receiver gathers.

Comparison of the stack of vibroseis data obtained through conventional NMO, common conversion point (CCP) stack and post-stack migration and the equivalent offset migration (EOM) stack of the same data show that the EOM method successfully produced a stack of comparable quality. The converted-wave velocity model derived through common scatter point analysis was similar to that obtained through semblance analysis of common conversion point gathers. Thus, EOM shows considerable promise as a method for converted-wave data velocity estimation and migration.

Joint PP-PS model-based inversion was only partially successful. The character ties between the migrated PS data and well data were not easy to make and the registration of the PP and PS data shows that the character match between the two datasets is poor. However, since we clearly have converted-wave data in this area, the dataset will be useful for testing converted-wave processing procedures such as velocity determination, statics estimation and migration, and PP-PS data matching and registration.

INTRODUCTION

In September, 2011, CREWES carried out an experimental low-frequency seismic shoot at Hussar, Alberta (Margrave et al, 2011). The line is 4.5 km long and runs NE-SW (Figure 1). Five source types were used and the data were recorded on six spreads with different receivers. In this paper, we discuss the processing and analysis of converted-wave data with vibroseis and dynamite sources recorded by 3C 10 Hz ARAM SM7 geophones. The vibroseis source was a custom-designed 1-100 Hz sweep that spent more time at the lowest frequencies. The dynamite source was 2 kg at a depth of 15 m. The sources were spaced 20 m apart and the receivers were spaced 10 m apart. Although the survey was acquired specially to record and investigate the processing of PP seismic data containing low frequencies in addition to those normally recorded, we also processed the converted-wave (PS) data.

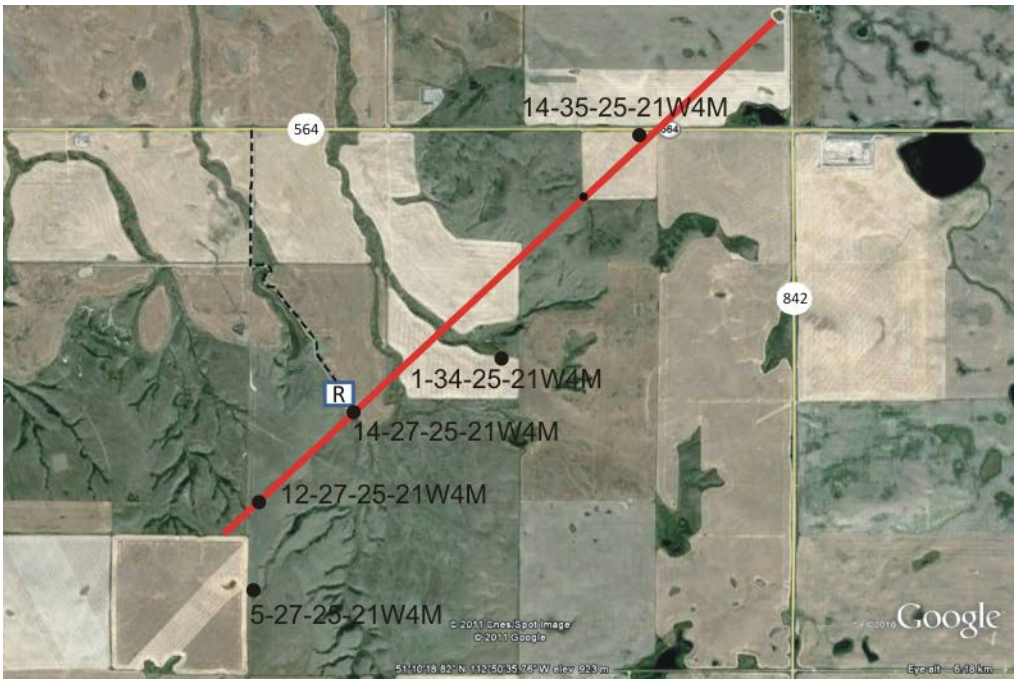

FIG.1: The orientation of the 2D line acquired at Hussar, Alberta in 2011.

SEISMIC DATA PROCESSING

The field data were separated into the three recorded components: vertical, inline and crossline. The 3C receivers were oriented magnetic east in the field so the inline and crossline data had to be rotated into the radial (source-receiver plane) and transverse (orthogonal to source-receiver plane) components (Tatham and McCormack, 1991) using equations (1).

$$R = I.\text{cosine}(\Theta) + X.\text{sine}(\Theta) \quad (1)$$

$$T = I.\ \text{sine}(\Theta - X.\ \text{cosine}(\Theta)$$

Where R denotes radial component, T denotes transverse component, I denotes inline component and X denotes crossline component. Θ (in radians) is the angle between the source to receiver azimuth minus the inline azimuth (magnetic east or 14.5° at Hussar in September 2011).

The radial components of the low dwell vibroseis and the dynamite data were processed using ProMAX. Figure 2 shows typical shot gathers from the two source types taken from the middle of the survey zoomed into the zone of interest within the first 3 seconds of data. There is noise from external sources apparent on both gathers around stations 230 and 530 and P-wave first break energy can be observed. Some converted-wave events show up fairly strongly on both source gathers around 1800 ms on stations 117-160. Elsewhere, any converted-wave energy is masked by the groundroll and noise. There appears to be no great problem with receiver statics, which would manifest themselves on shot gathers as disruptions in the moveout of observed reflections.

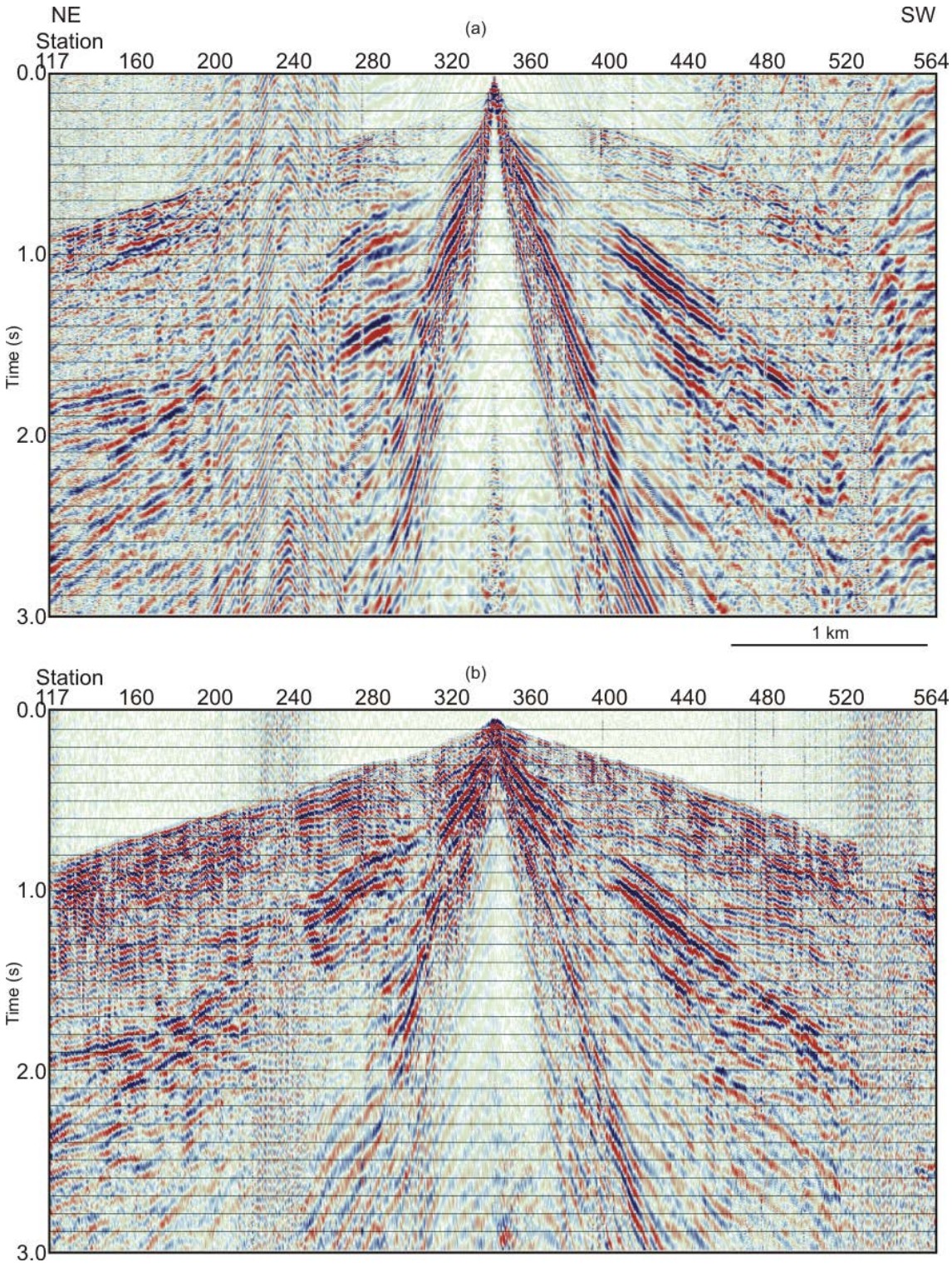

FIG. 2: Sample shots from the radial component of the (a) vibroseis data and the (b) dynamite data. Although 10 s of data were recorded we show the zone of interest within the first 3 s. The line runs from NE on the left to SW on the right.

We applied a series of radial filters (Henley, 1999; 2011) to receiver gathers specifically to attenuate high amplitude noise trains with velocities significantly lower than the expected converted-wave energy. We did not want to attenuate any of the desired reflections. The velocities we targetted were between 200 m/s and 470 m/s. After application of the radial filters, we applied an air blast attenuation and surface wave noise attenuation on shot gathers to remove some remaining undesired surface wave energy. Figure 3 shows the same shot gathers as in Figure 2 after radial filtering, air blast and surface wave noise attenuation.

To calculate receiver statics, we created a receiver stack (Harrison, 1992). The input vibroseis receiver gathers had radial filtering and surface wave noise attenuation applied, shot statics and NMO estimated from preliminary velocity analysis of the PS data. A horizon was picked and we tested calculation of the receiver statics by two ways: (1) the receiver statics are the difference between the picked horizon and this horizon flattened at 1600 ms (2) the receiver statics are the difference between this horizon and a smoothed version of it. It has been shown that the amount of smoother applied can have a surprising effect on the continuity of reflections in the final CCP stacks (Isaac and Margrave, 2011). The data were binned to common conversion points using Vp/Vs of 2.15, which was derived from compressional- and shear-wave sonic log data from well 12-27-25-21W4M. Figure 4 displays the CCP stacked data with receiver statics calculated by the two methods. These stacks show that the statics calculated using a flattened horizon (Figure 4a) have worked better on this dataset. We then applied another round of residual receiver statics. The values of the total receiver statics is shown in Figure 5 with the PP receiver statics plotted for comparison.

After determination of the receiver statics we applied predictive deconvolution to the shot gathers. The data were binned asymptotically into common conversion points (CCP) (Tessmer and Behle, 1988) using Vp/Vs of 2.15, stacked and poststack time migrated using a finite difference algorithm. Figure 6 shows the migrated CCP stacks with a bandpass filter of 5-10-100-120 Hz and an fx deconvolution applied. There appears to be some unfiltered noise remaining in the dynamite data. However, both stacks show good converted-wave reflections. For comparison of migration techniques applied to the same filtered data, we show in Figure 7 the PS vibroseis data migrated using the prestack EOM migration. For a full description of the velocity analysis and EOM migration, see Guirigay and Bancroft (this volume). The EOM data appear smoother and there are migration artefacts at the sides. No fx deconvolution or bandpass filters were applied to the EOM data.

The converted-wave stacking velocities were obtained through standard semblance analysis of CCP supergathers. We used a single averaged velocity for the final stacked section. Figure 8 shows this velocity and the single migration velocity used by Guirigay and Bancroft (this volume), which was derived through analysis of data binned into common scatter points (CSP). The two velocity functions are quite similar, suggesting that the CSP method of analysis is useful for converted-wave velocity analysis. The CSP method could be especially useful when the converted-wave data are poor and semblance velocities hard to pick.

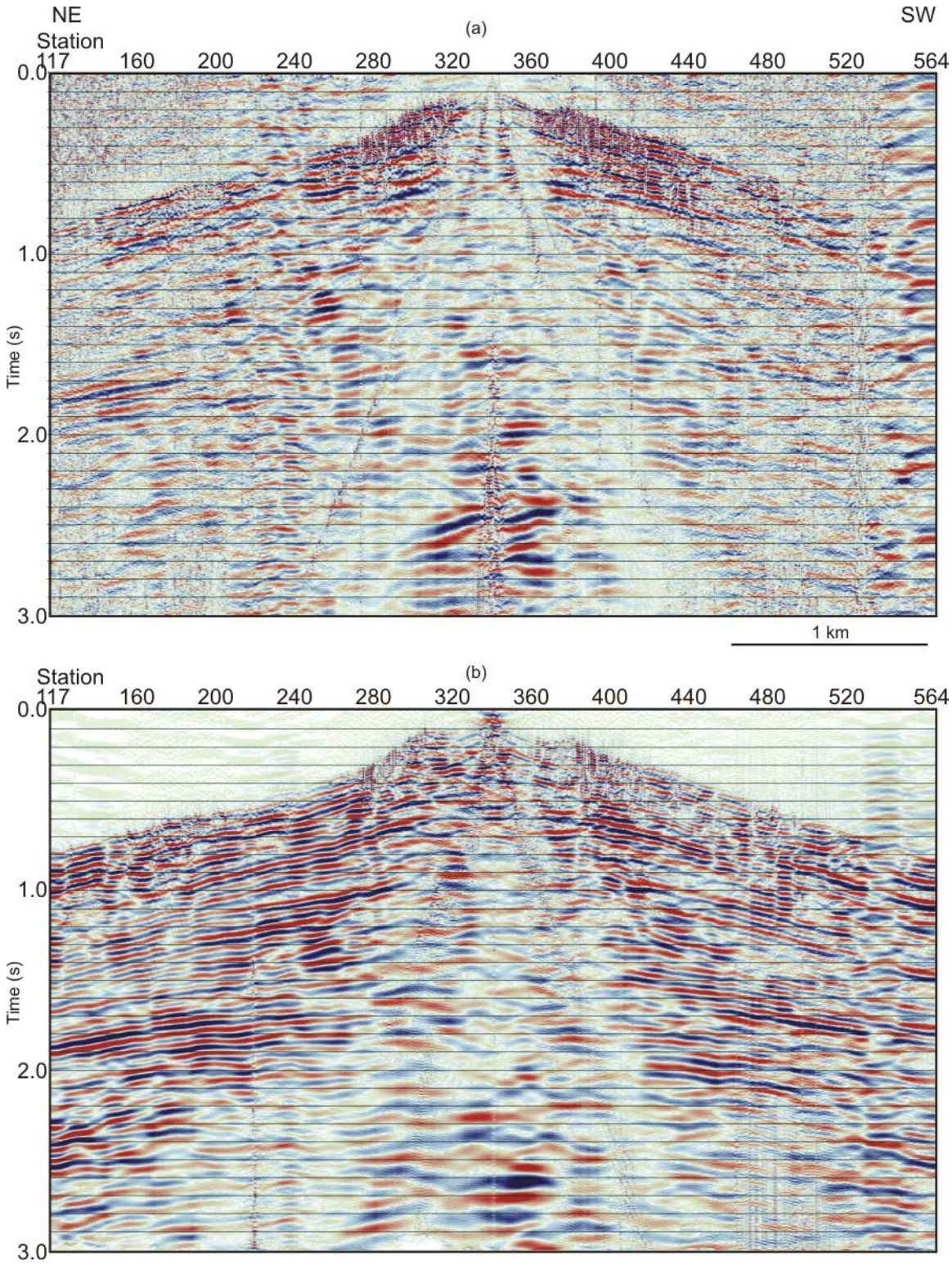

FIG. 3: Shots from the radial component of the (a) vibroseis data and the (b) dynamite data after application of radial filters, air blast attenuation and surface wave noise attenuation.

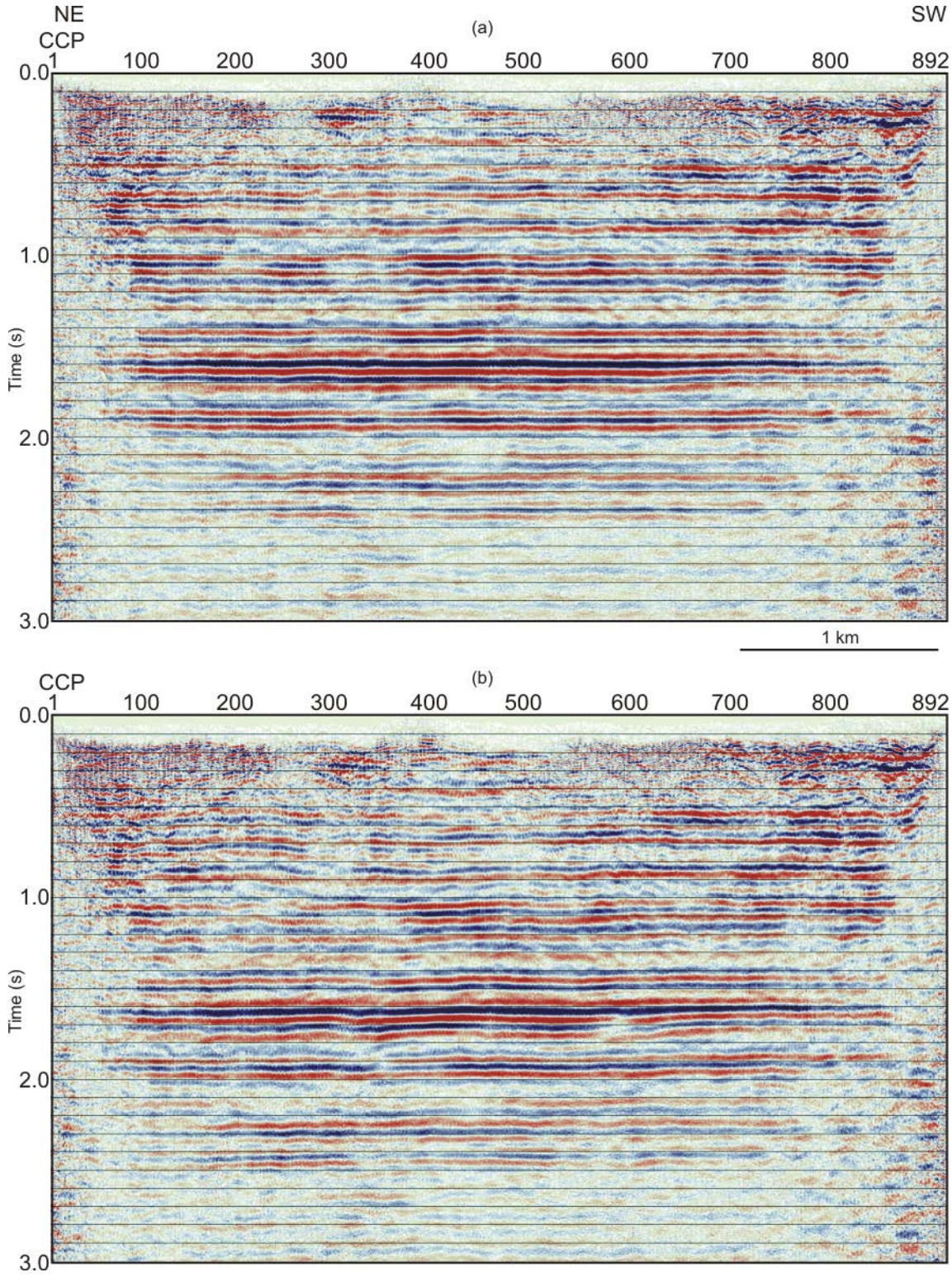

FIG. 4: CCP stacks with the first pass of receiver statics calculated by subtracting from the picks of an horizon near 1600 ms the flattened (a) and smoothed (b) versions of those picks.

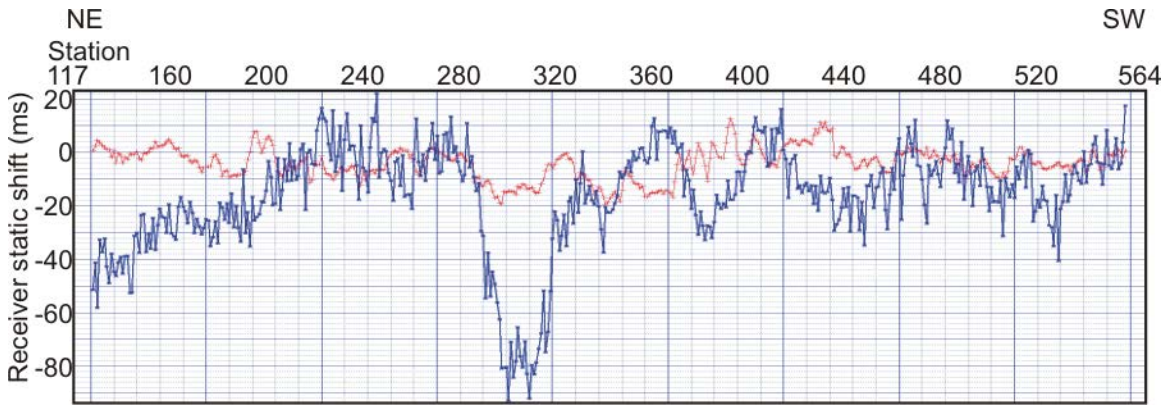

FIG. 5: The PS receiver statics (in blue). For comparison the PP receiver statics are also plotted (in red).

SEISMIC DATA INVERSION

We registered the PP and PS post-stack migrated data using compressional and shear sonic logs and density logs from well 12-27-25-21W4M. Because the location of this well falls on the seismic section in an area of inadequate fold we shifted the well laterally by 500 m to where the fold is higher to be able to make a better tie between the synthetic seismograms and seismic data. The well-PP tie is shown in Figure 9 and the well-PS tie in Figure 10. We based the tie primarily on the correlation between the synthetic and seismic data of the Lea Park and Viking reflections. Below the top of the Mannville Formation the character match is poor for the PP data. After tying the PP and PS data to the well we picked horizons on both sections and registered the two datasets. Figure 11 shows the PP and PS data both displayed in PP time with the registered horizons. The character match between the two sections is not good but it is the best we could do with the current processed data.

A joint PP-PS model-based general linear inversion using Hampson-Russell's ProMC software was only partially successful for undetermined reasons. The initial model for input into the inversion was derived from the P and S sonic logs of well 12-27-25-21W4M, which were correlated with both the PP and PS data. The data nearest the well locations inverted successfully but further away traces that inverted were intermixed with traces that did not. For the part of the section over which the inversion succeeded, we show the original Vp/Vs model calculated from the 12-27-25-21W4M well logs (after being tied to the seismic data) in Figure 12a and the inverted Vp/Vs in Figure 12b. The inversion shows some lateral changes in Vp/Vs derived from the PP and PS data character through inversion.

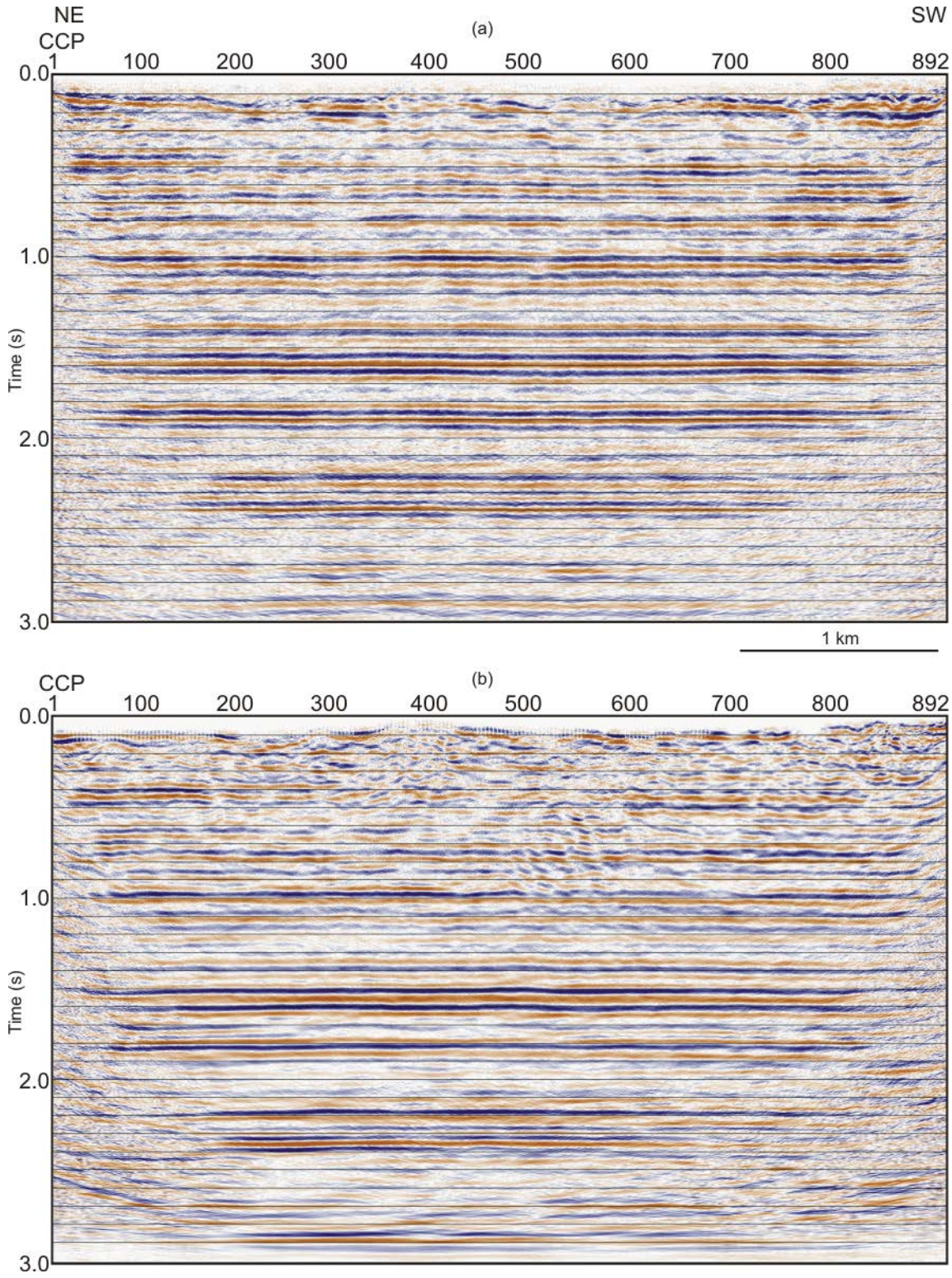

FIG. 6: Poststack migrated CCP stacks of the (a) vibroseis and (b) dynamite PS data.

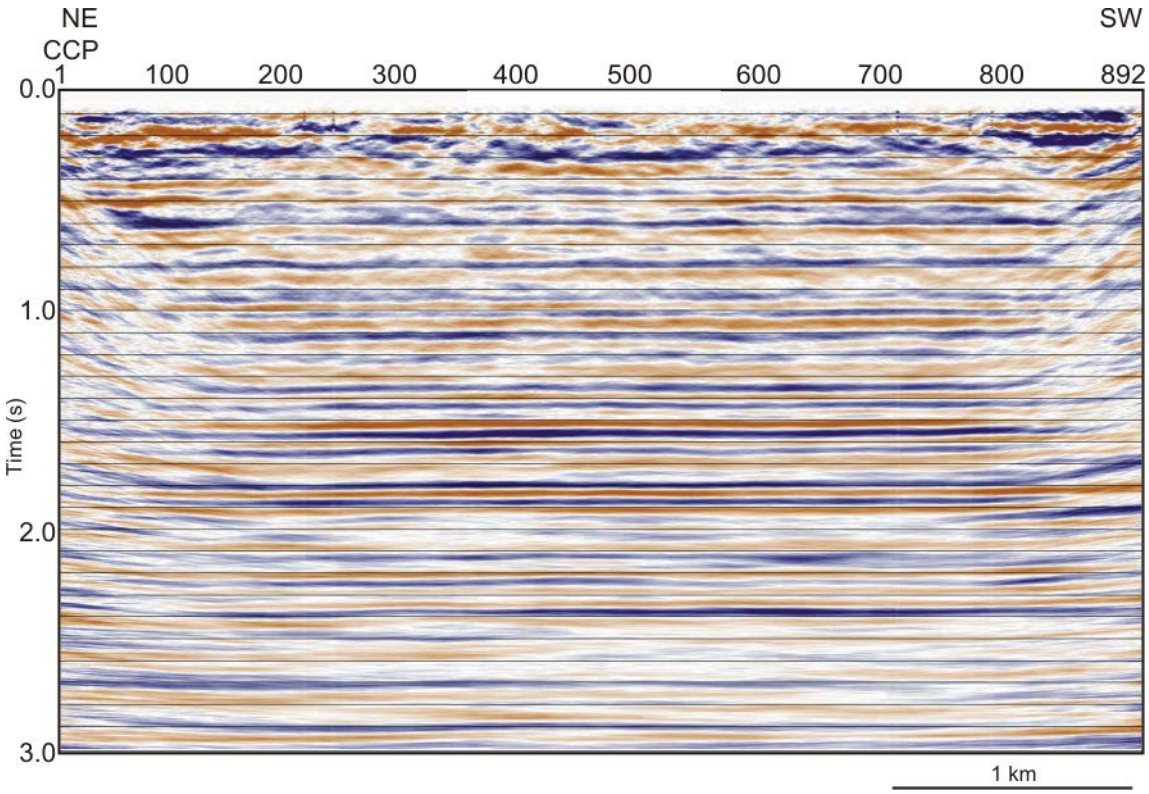

FIG. 7: The vibroseis PS data migrated using EOM. These data are processed to a slightly lower datum than the migrations in Figure 6. Compare to Figure 6a, which is the poststack FD migrated version.

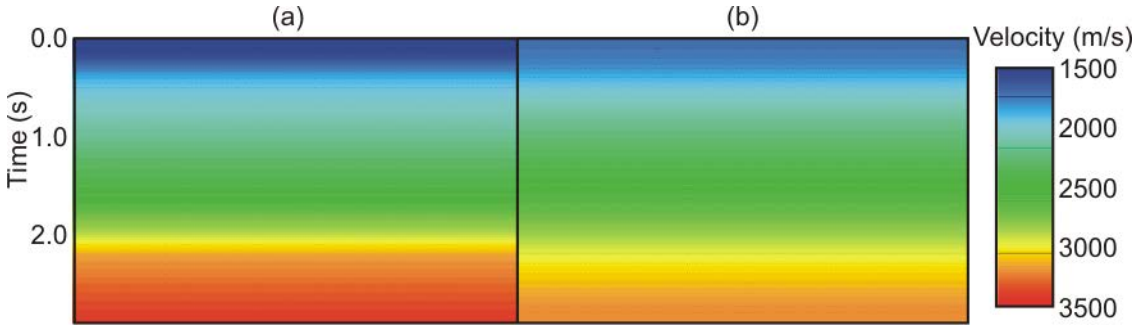

FIG. 8: (a) Averaged converted-wave stacking velocity derived through semblance analysis of common converted point data compares well with (b) EOM velocity derived through common scatter point data analysis.

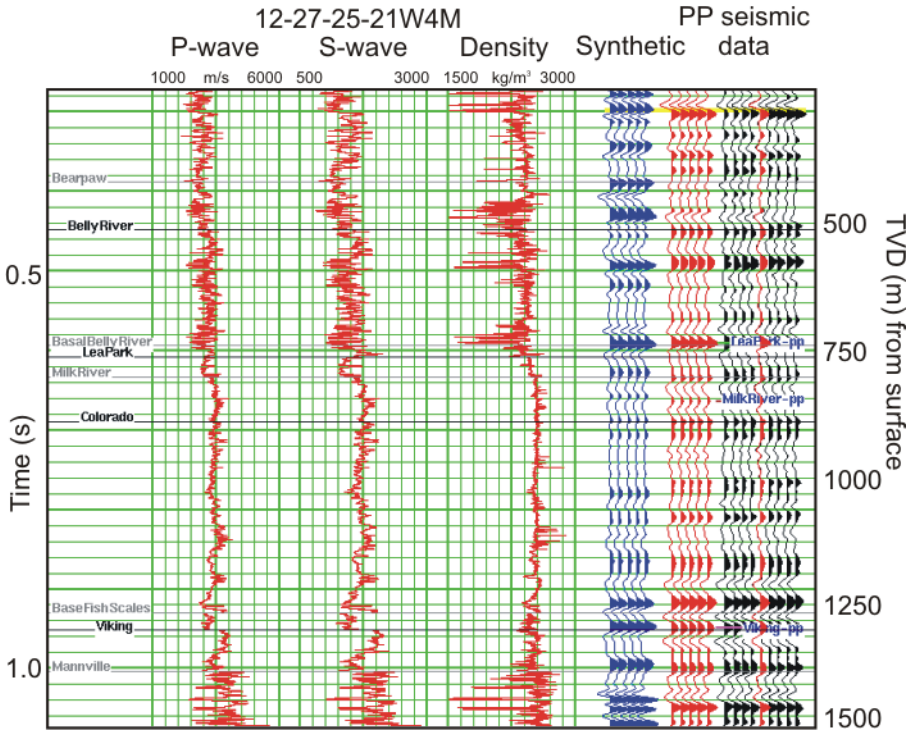

FIG. 9: Tie between well 12-27-25-21W4M and the PP seismic data. The correlation is based primarily upon character matches of the Lea Park and Viking reflections.

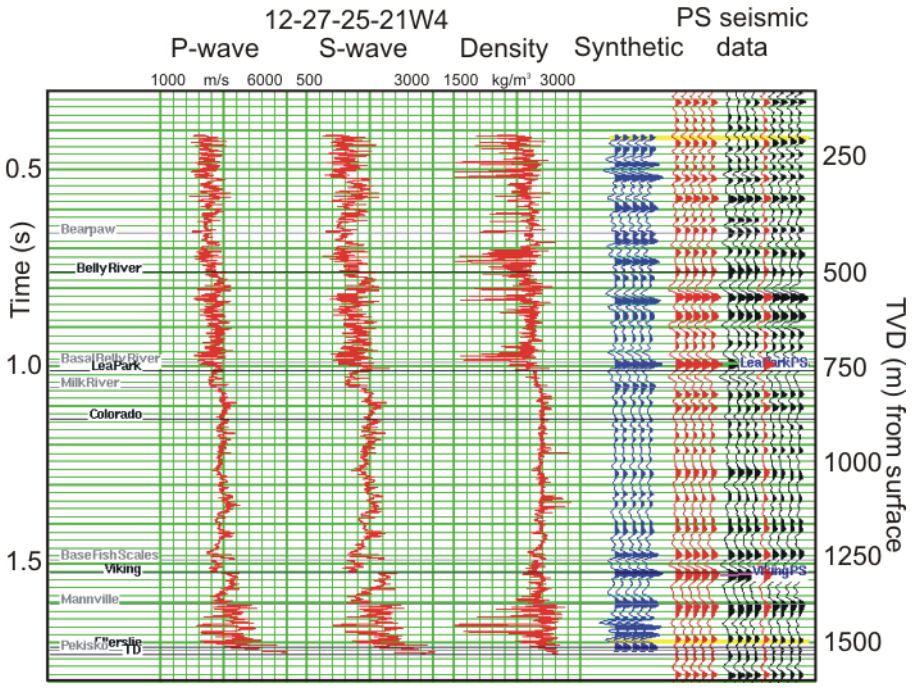

FIG. 10: Tie between well 12-27-25-21W4M and the PS seismic data. The correlation is based primarily upon character matches of the Lea Park and Viking reflections.

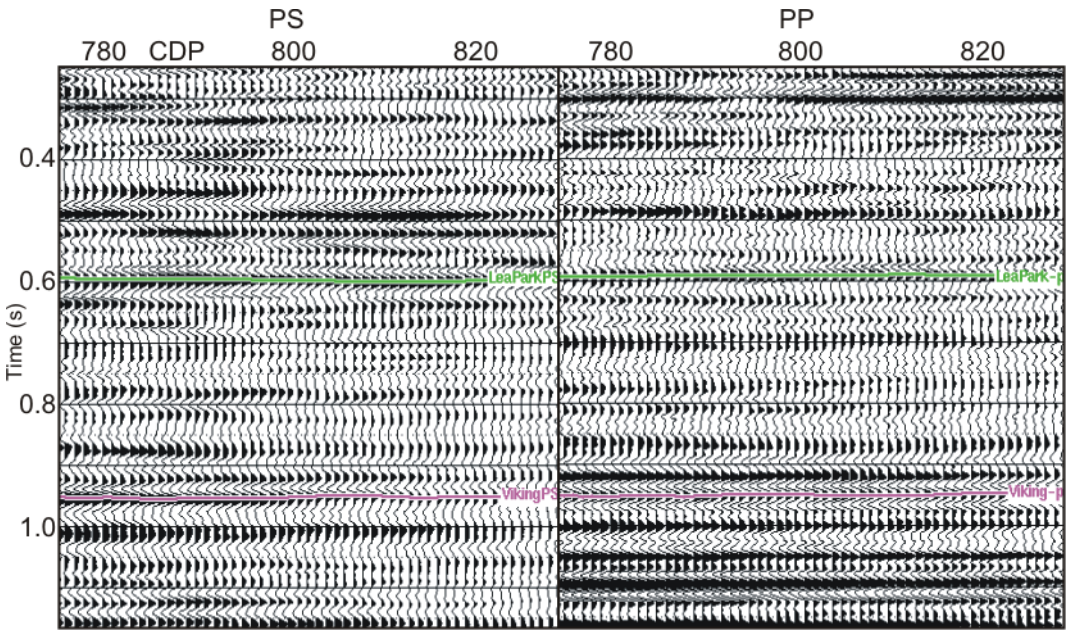

FIG. 11: Registered PS and PP data with the correlated horizons. The PS data have been scaled to PP time.

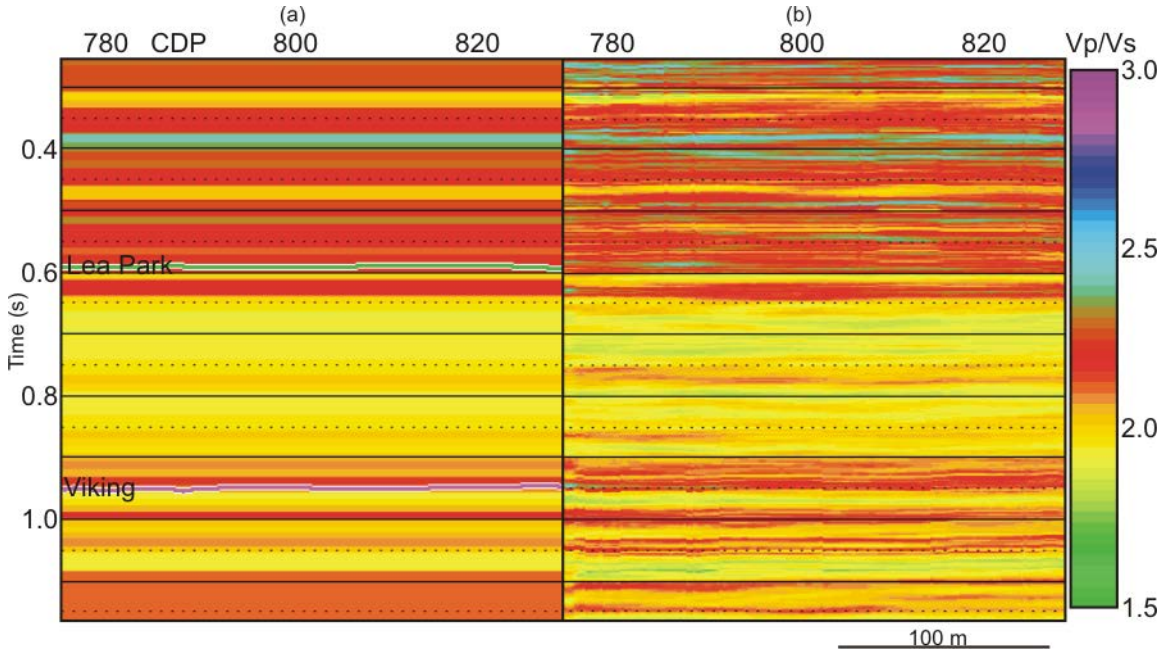

FIG. 12: (a) Initial Vp/Vs model derived from the well 12-27-25-21W4M and the registered PS and PP sections (Figure 11), and (b) the inverted Vp/Vs. Only the part of the line where the inversion was successful is shown.

DISCUSSION

Converted-wave data were recorded successfully at Hussar. We processed data with both dynamite and vibroseis sources. The EOM method successfully produced a stack of vibroseis data comparable in quality to that obtained through conventional NMO, CCP stack and post-stack migration. The converted-wave migration velocity was comparable to the stacking velocity derived through semblance analysis. Thus, we believe that converted-wave EOM shows considerable promise as a method for converted-wave data velocity estimation and migration.

Joint PP-PS inversion was only partially successful and we are unsure why. The character ties between the migrated PS data and well data were not easy to make and the registration of the PP and PS data shows that the character match between the two datasets is poor. Further work could be done to process the datasets so that the character match is better.

The converted-wave data is of good quality thus will be useful for testing converted-wave processing procedures such as velocity determination, statics estimations, and migrations.

ACKNOWLEDGEMENTS

We thank the CREWES sponsors for their generous support. We acknowledge Landmark Graphics Corporation for ProMAX, and CGGVeritas for the Hampson-Russell software Geoview, with which we did the inversion.

REFERENCES

Isaac, J. H. and G. F. Margrave, 2011, The effect of receiver statics on CCP stacks: An example from Spring Coulee, Alberta: CREWES Research Report Vol. 23.

Guirigay, T. A. and J. C. Bancroft, 2012, P-S migration using equivalent offset method: CREWES Research Report Vol. 24.

Harrison, M. P. 1992, Processing of P-SV surface seismic data: Anisotropy analysis, dip moveout and migration: Ph. D. thesis, University of Calgary.

Henley, D. C., 1999, Coherent noise attenuation in the radial trace domain: Introduction and demonstration: CREWES Research Report, Vol. **11**, Ch. 36.

Henley, D. C., 2011, Now you see it, now you don't: radial trace filtering tutorial: CREWES Research Report Vol. 23.

Margrave, G. F., L. Mewhort, T. Phillips, M. Hall, M. B. Bertram, D. C. Lawton, K. Innanen, K. W. Hall and K. Bertram, 2011, The Hussar low-frequency experiment: CREWES Research Report Vol. 23.

Tatham, R. H. and M. D. McCormack, 1991, Multicomponent seismology in petroleum exploration: SEG Investigations in Geophysics Vol. 6.

Tessmer, G. and A. Behle, 1988, Common reflection point data-stacking technique for converted waves: Geophysical Prospecting, 36, 671-688.